

Advanced Optical-Label Routing System Supporting Multicast, Optical TTL, and Multimedia Applications

Zhong Pan, *Student Member, IEEE, Student Member, OSA*, Haijun Yang, *Student Member, IEEE*, Jinqiang Yang, Junqiang Hu, Zuqing Zhu, *Student Member, IEEE, Student Member, OSA*, Jing Cao, *Student Member, IEEE*, Katsunari Okamoto, *Fellow Member, IEEE*, Satoru Yamano, *Member, IEEE*, Venkatesh Akella, *Member, IEEE*, and S. J. Ben Yoo, *Senior Member, IEEE, Member, OSA*

Abstract—This paper reports on modern features of the optical-label switching (OLS) system in support of multicast, optical time-to-live (TTL), and video-streaming applications. We first propose and demonstrate optical-label switching core router architecture with multicast function. The multicast switching architecture provides reduced complexity and effective multicast contention resolution compared to conventional multicast-capable switching fabric. A proof-of-principle experiment successfully showed packet multicast forwarding with contention resolution. The all-optical TTL monitors the healthiness of the packet, and prevents degraded packets from traveling or looping further in the network. The experiment demonstrated successful packet discards based on optical signal-to-noise ratio degradation. Finally, we present an optical label switching edge router that supports aggregation, quality of service, and class of service, and we further demonstrate a video streaming application between Ethernet clients through the OLS edge routers and a core router. The modern features of OLS routers proposed and demonstrated in this paper indicate the viability of OLS technologies in future photonic Internet in support of modern applications.

Index Terms—Contention resolution, core router, edge router, Fast Ethernet, multicast, optical label switching (OLS), optical packet switching (OPS), optical performance monitoring, time to live (TTL), video streaming, wavelength conversion.

I. INTRODUCTION

THE internet traffic continues to grow very rapidly at an accelerating pace while its service applications are becoming extremely diverse. Emerging voice-over-IP, packet video, and peer-to-peer file transfer services are adding to traditional Internet services. While the accelerating capacity demands have been successfully met by wavelength-division multiplexing (WDM) based high-bandwidth optical circuit-switching (OCS) technologies in the core network, optical packet switching (OPS) [1] can readily transport packetized data and support the diverse services with high capacity utilization. Optical label

switching (OLS) [2] allows seamless interoperability with OPS, OCS and optical burst switching (OBS) on a WDM platform [3]. Furthermore, OLS facilitates support for quality of service (QoS), class of service (CoS), type of service (ToS), and traffic engineering [3]. Recently demonstrated optical label switching routers showed promising capabilities including variable-length packet switching with all-optical contention resolution [4], cascaded 11-stage packet forwarding [5], IP-client-to-IP-client packet transport with OLS edge routers [6], and a 477 km field fiber network trial [7]. Building upon successful demonstrations of OLS routers, it is now important to address modern features of OLS core and edge routers.

This paper addresses modern features of OLS routers geared towards supporting diverse services of the future photonic Internet. We will discuss theoretical and experimental demonstrations of three main features.

The first is the multicast OLS core router with multicast contention resolution. Future all-optical Internet is expected to support diverse services including multimedia streaming and conferencing applications requiring multicast. The multicast-capable core routers require far less network capacity than unicast core routers to support multicast applications, and consequently, multicast is a desirable feature in optical core routers. All-optical contention resolution and arbitration in multicast-capable optical routers rise as a challenging issue since multicast brings increased level of contention probabilities. We will discuss the multicast-capable switching fabric architecture, the multicast contention resolution algorithm, the network performance simulation results, and the multicast OLS router experimental demonstrations.

The second is optical time-to-live (TTL). While the conventional TTL scheme simply decrements the TTL value by one at each hop [8], [9] in conventional data networks in order to mitigate routing loops, it is desirable if the all-optical data networks consider “optical-TTL” which performs weighted TTL decrementation considering both router hops and optical transmissions. The optical-TTL based on the optical signal-to-noise-ratio (OSNR) monitors the signal quality of the packet in real time and drop seriously deteriorated packets. This method takes into account the transmission quality variation on different fiber spans and systems in addition to signal degradations after passing cascaded stages of switching systems, thus it serves the goal to remove “stale” packets from the network by monitoring the healthiness of each packet. It also provides a means to achieve packet-by-packet performance monitoring using

Manuscript received December 30, 2004. This work was supported in part by National Science Foundation Advanced Network Infrastructure (NSF ANI) 9986665, National Science Foundation Network Research Testbeds (NSF NRT) 0335301, and Optoelectronics Industry Development Association Photonics Technology Access Program (OIDA PTAP), which is supported by NSF and Defense Advanced Research Projects Agency Microsystems Technology Office (DARPA MTO).

Z. Pan, H. Yang, J. Yang, J. Hu, Z. Zhu, J. Cao, V. Akella, and S. J. Ben Yoo are with the Department of Electrical and Computer Engineering, University of California, Davis, CA 95616 USA (e-mail: yoo@ece.ucdavis.edu).

K. Okamoto is with the Okamoto Laboratory, Ltd., Ibaraki 310-0035, Japan.

S. Yamano is with System Platforms Research Laboratories, NEC Corporation, Nakahara-ku, Kawasaki, Kanagawa 211-8666, Japan.

Digital Object Identifier 10.1109/JLT.2005.855682

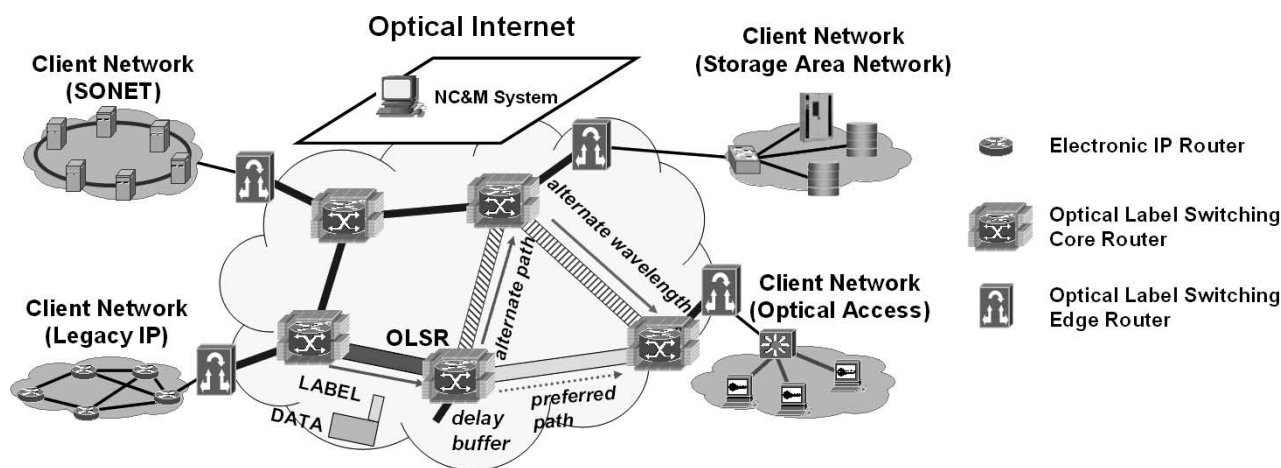


Fig. 1. OLS network architecture consisting of OLS core routers, edge routers, and an NC&M system. NC&M: network control & management; SONET: synchronous optical network; OLSR: optical-label switching router.

optical-labels [10], [11]. Here we discuss a proof-of-principle experimental demonstration of packet discard using optical-TTL across modern OLS core routers.

Lastly, we discuss a modern OLS edge router capable of label generation and packet classifications based on QoS/CoS/ToS, and packet aggregation. Xue *et al.* [12] have demonstrated in detail the importance of packet aggregation that resulted in traffic shaping and low packet loss rates for a given normalized load level. Further, forward-equivalent-class (FEC) classifications based on QoS, CoS, and ToS parameters, resulting FEC based queuing, and corresponding optical label generation are important aspects of the OLS edge router. In this paper, we design and demonstrate operation of the OLS edge routers with the OLS core routers to achieve successful video-streaming application from IP-client to IP-client across the OLS network.

This paper is structured as follows. Section II discusses the OLS network and system architecture, focusing on the OLS core router architecture supporting multicast and optical-TTL, and the edge router architecture with packet aggregation as well as QoS/CoS/ToS support. Section III presents the experimental demonstrations of an OLS core router with multicast support; an optical-TTL scheme; and an end-to-end video streaming with Ethernet clients, OLS edge routers and OLS core router. Section IV summarizes the paper.

II. OLS NETWORK AND SYSTEM ARCHITECTURE

The OLS technology will greatly simplify the optical network by removing the intermediate synchronous optical network (SONET) and asynchronous transfer mode (ATM) layers. IP over OLS over WDM enables an efficient utilization of the optical bandwidth. Moreover, OLS is compatible with the legacy WDM technology. An in-band labeling scheme allows the label to travel with the payload on the same transmission wavelength, leaving other wavelength channels in the same fiber untouched. From the network point of view, OLS seamlessly supports OPS, OBS and OCS [3]. The flexibility of the optical label makes the dynamic support of QoS, CoS and ToS possible [3]. In addition, the optical label enables schemes for performance monitoring [10], [11] and optical-TTL. Combin-

ing the optical-label signaling and supervisory channels, OLS Network Control and Management (NC&M) can perform auto-discovery, auto-configuration and auto-restoration of the OLS network [3].

Fig. 1 shows an OLS network composed of OLS core routers, edge routers and an NC&M system. Optical labeling schemes compatible with OLS include bit-serial, label-wavelength, optical-subcarrier modulation (SCM), and orthogonal-modulation [13], [14] methods. The OLS system in this paper utilizes both the SCM labeling and bit-serial labeling. Both schemes enable the label to travel with the payload on the same transmission wavelength, and both are capable of all-optical label swapping without the bulky and inefficient O/E/O conversion for the payload. SCM labeling facilitates an easier removal of the label by optical filtering [15], while a bit serial label can survive all-optical wavelength conversions based on intensity modulation, such as the cross-gain modulation (XGM) or cross-phase modulation (XPM) in a semiconductor optical amplifier (SOA).

Fig. 1 depicts packet switching with SCM labeling over the OLS network. The ingress edge router receives legacy format packets from a source client network, and performs packet aggregation according to QoS/CoS parameters and packet arrival statistics. Packet aggregation can effectively smooth out the variations in the optical packet size distribution and achieve traffic shaping [12]. Then the edge router generates the optical label content based on the destination, QoS/CoS/ToS parameters, the optical-TTL initial value, and other information pertaining to routing decision. The TTL is a necessary feature to mitigate the routing loop problem. An optical-TTL can further monitor the payload signal quality degradation induced by the transmission and switching. Finally, the label and payload are modulated onto the optical carrier by the labeling scheme used, such as the SCM labeling shown here. Each intermediate OLS core router reads the information from the optical label while keeping the payload in the optical domain. If the optical-TTL attached to the packet has expired, the router will drop this packet. Based on the label information and the routing table, the router switches the packet to its next hop. If the packet is marked for multicast, according to the multicast tree

the router may need to duplicate the packet into multiple copies and forward them to multiple next hops. The router may or may not perform label swapping, depending on the labeling scheme and the OLS network design [3]. When it does, it will update the optical-TTL field inside the label. Finally, the egress edge router removes the label, restores the legacy packet format, and delivers the packet to the destination client network.

The following subsections will first discuss the architecture of the OLS core router that supports multicast. In particular, we propose two multicast contention resolution schemes and compare their performance through simulation. Then we will discuss the optical-TTL scheme used in the OLS network. Finally we will present the architecture of the OLS edge router with packet aggregation, QoS/CoS/ToS support, and versatile client network support. These three aspects are the important modern features in the recent progress of the OLS network and system research.

A. OLS Core Router Architecture Supporting Multicast

Multicast in an all-optical router is challenging due to the absence of optical logical circuits and buffers to generate copies of multicast packets. Previously reported architectures include broadcast-and-select structures and one-to-many (multi-) wavelength conversion based structures [16]. Switching fabrics with broadcast-and-select structures suffer from excessive losses, because each signal power has to be split into at least N streams, where N is the number of possible multicast destinations [17]. Moreover, the number of switching elements required is extremely large, typically on the scale of N^2 since N switching elements are required for each of the N ports. Multi-wavelength conversion [18]–[21] based architectures providing simultaneous multiple copies of an incoming signal avoids excessive losses (“ $1/N$ loss”). However, a non-blocking multicast switch is, again, overly complicated since it requires a large number of active components [16].

We propose a switching architecture with a limited multicast function, in which a limited number of linecards are responsible for multicast traffic while leaving unicast traffic switched in the original way as described in the previously reported OLS router switching fabric architecture [12]. Hence, by providing a limited number of extra port(s) in the original switch fabric, the OLS core router is capable of handling multicast packets while supporting unicast packets as in the original architecture.

Fig. 2 illustrates this concept. This figure shows an OLS router switching architecture example with four input fibers and four output fibers, each carrying two wavelengths. The third fiber port is a fixed-length delay line that acts as an optical buffer to support the time-domain contention resolution scheme [4]. The fourth fiber port is the multicast port. When a multicast packet arrives at the router through the first or the second input fiber port, the switch control will send it to the multicast port, where it is duplicated by the multi-wavelength converter (MWC) onto multiple wavelengths that will direct it to multiple output ports of the arrayed waveguide grating router (AWGR). This way, the proposed architecture supports both unicast and multicast without bulky and lossy broadcast-and-select structures that typically require a far greater number

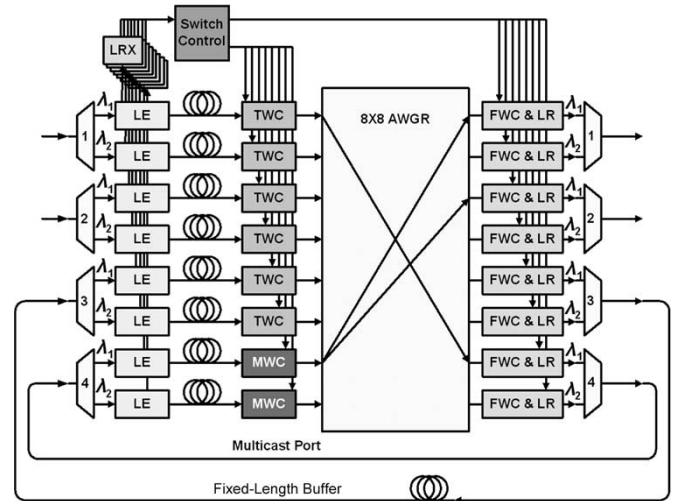


Fig. 2. Simplified architecture of an OLS core router with multicast support. The arrows show the possible trace of a multicast packet. LE: label extractor; LRX: label receiver; TWC: tunable wavelength converter; AWGR: arrayed waveguide grating router; MWC: multiwavelength converter; FWC & LR: fixed wavelength converter and label rewriter.

of active components (lasers, gates, and switches). The proposed architecture accompanies “multicast port contention” in addition to “output port contention” due to the limited number of multicast ports. When multicast packets occupy all the multicast ports, the switching fabric will not be able to support additional multicast packets. This prevents the router from supporting pure multicast traffic in which all or vast majority of the incoming packets require multicast. If the multicast traffic consistently occupies a large portion of the total traffic to result in high multicast-contention rates, the switching fabric can add additional multicast ports or upgrade existing unicast linecards to multicast linecards.

All-optical contention resolution schemes in wavelength, time, and space domains, as discussed in detail in [12] for unicast traffic, must take multicast contention resolution into consideration. The following two schemes are discussed in this paper.

Multicast Contention Resolution Scheme 1 (MCAST1): Multicast contention resolution scheme 1 (MCAST1) is a straightforward derivation of the unicast contention resolution scheme. It consists of five steps in resolving both the multicast port contention and each destination output port contention as shown in Fig. 3. The switch control adopts the following steps to schedule the incoming multicast packet P .

- Step 1) The switch control forwards the multicast packet from the input port to one of the multicast ports. In this step, if multiple multicast packets are contending for the same wavelength on the same multicast port, the wavelength domain contention resolution method is used in resolving the multicast port contention.
- Step 2) If all wavelength channels on all multicast ports are occupied, the switch control attempts the time domain contention resolution, i.e. to switch the multicast packet to one of the fiber delay line (FDL) ports for buffering.

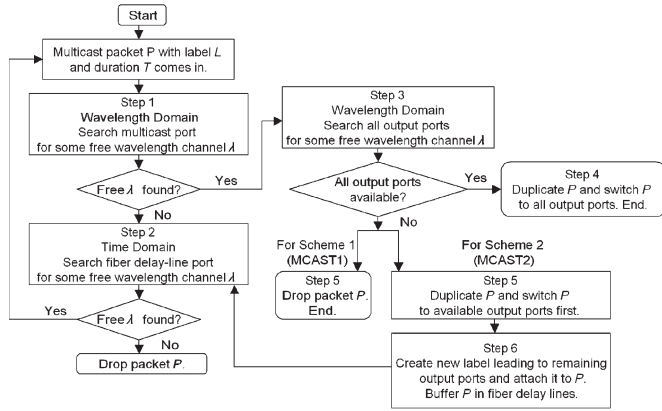


Fig. 3. Multicast contention resolution scheme 1 (MCAST1) and scheme 2 (MCAST2).

- Step 3) If the multicast packet is switched to one multicast port successfully, the switch control will check the availability of all desired output ports simultaneously while employing the wavelength domain contention resolution in resolving the contention for any specific wavelength on each output port.
- Step 4) If all desired output ports are available at the same time, the MWC at the multicast port will duplicate the packets onto multiple wavelengths that will forward the copies through the AWGR to multiple desired output ports.
- Step 5) Otherwise, the multicast packets will be dropped.

For *MCAST1*, the successful resolution of contention will require that each destination port must have at least one free wavelength channel at the same time. For network nodes with high degrees of connectivity, the probability of blocking for the multicast packet could be high.

Multicast Contention Resolution Scheme 2 (MCAST2): The six-step multicast contention resolution scheme 2 (*MCAST2*) is proposed to further improve the multicast-capable router performance as shown in Fig. 3. *MCAST2* employs the same Steps 1–4 as *MCAST1*, but differs on the fifth step, where *MCAST2* uses both the wavelength domain and the time domain contention resolution methods in resolving each destination output port contention for individual multicast packets. It follows the following six steps.

- Steps 1–4) are the same as *MCAST1*.
- Step 5) If some but not all desired output ports are available simultaneously, the switch control will duplicate the packet and forward the copies to the available output ports first.
- Step 6) Then the switch control assigns a new label to an additional copy of the multicast packet. This label will lead the packet to the fiber delay line buffer, and attempt to forward the packet to the remaining desired output ports at a future time.

This way, the multicast contention resolution scheme 2 (*MCAST2*) does not require all of the destination ports to be free at the same time and avoids the situation when one (or a limited number of) busy output port(s) blocks the entire

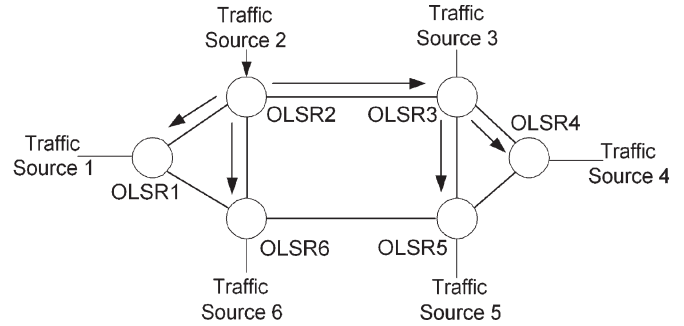


Fig. 4. Simulation-networks setup to study the performance of the multicast contention-resolution schemes.

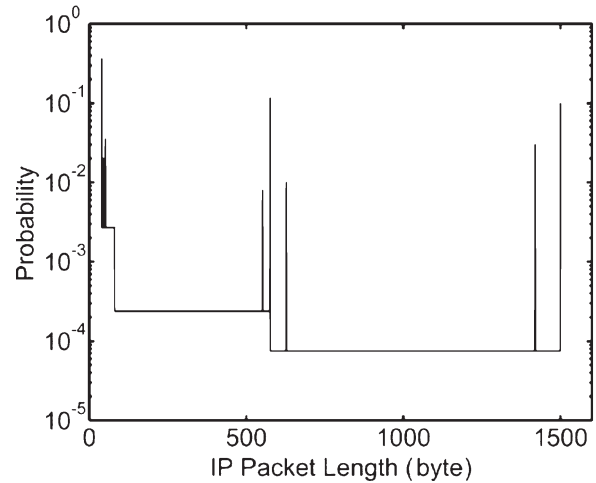


Fig. 5. IP packet-length distribution used for simulations.

multicast session. It leads to a lower blocking probability even for nodes with high degrees of connectivity.

We compare the performance of the two multicast contention resolution schemes through a simulation driven by the self-similar traffic. This work adopts a self-similar model called “Sup_FRP” [22] to generate packet traces with Hurst parameter $H = 0.8$. Fig. 4 shows a six-node OLS network where each WDM fiber link is bi-directional and carries multiple wavelengths transmitting at 2.5 Gb/s with uniform background traffic. Each node denotes a multicast-capable OLS router with one traffic source (client) that generates IP packets with a realistic IP packet length distribution. Fig. 5 shows this distribution [23] with the average packet size of 404.5 bytes, the maximum packet length of 1500 bytes, and the minimum packet length of 40 bytes. Multicast packets from traffic source 2 enter node 2 with their destinations set for node 4, node 5, node 6, and node 1 respectively. The arrows in Fig. 4 show the multicast tree, based on which node 2 and node 3 forward incoming multicast packets to their destinations.

Switch fabric simulation configurations are listed in Table I, where *MCAST1-1FDL* and *MCAST1-2FDL* denote the multicast OLS router using multicast contention resolution scheme 1 equipped with one and two fiber delay lines respectively, whereas *MCAST2-1FDL* and *MCAST2-2FDL* denote the multicast OLS router using multicast contention resolution scheme 2 with one and two fiber delay lines respectively.

TABLE I
SIMULATION CONFIGURATIONS

Type	Port	Channel	Switch Size	Multicast Port	Fiber Delay Lines
MCAST1-1FDL	5 × 5	4	20 × 20	1	1
MCAST1-2FDL	6 × 6	4	24 × 24	1	2
MCAST2-1FDL	5 × 5	4	20 × 20	1	1
MCAST2-2FDL	6 × 6	4	24 × 24	1	2

Fig. 6 shows the simulation results, where the load of the local transmitter, defined as the ratio between the total numbers of bits offered per unit time and the line-speed, varies from 0.3 to 0.7 in the simulation. Fig. 6(a)–(c) show simulated packet loss rates, forwarding delays, and timing jitter of the above four cases with a given multicast traffic percentage of 10%.

Packet Blocking Rate Analysis: Fig. 6(a) demonstrates that multicast contention resolution scheme 2 (*MCAST2*) achieves lower packet loss rate than scheme 1 (*MCAST1*) for a given traffic load and a given number of fiber delay lines, indicating that scheme 2 resolves contention more effectively. In addition, the increase of the number of fiber delay lines from 1 to 2 in scheme 2 results in more significant decreases in the packet loss rate than in scheme 1 for a given traffic load.

Average Packet-Forwarding Delay and Jitter Analysis: The forwarding delay in each node is mainly introduced when the packets go through the fiber delay line buffer. Fig. 6(b) shows that multicast contention resolution scheme 2 (*MCAST2*) achieves lower forwarding delay than that for scheme 1 (*MCAST1*) for a given number of fiber delay lines and traffic load. It also shows that the forwarding delay increases as the number of fiber delay lines increases from 1 to 2. This is because more contending cases are resolved by fiber delay lines, which leads to a larger average packet forwarding latency. Fig. 6(c) shows that the average forwarding jitter increases slower in multicast contention resolution scheme 2 compared to scheme 1, as the traffic load increases. Fig. 6(a)–(c) demonstrate that the multicast contention resolution scheme 2 has superior OLS network performance compared to the scheme 1 in terms of the packet loss rate, forwarding delay, and jitter.

Section III-A presents an experimental demonstration of the proposed multicast architecture using a simple contention resolution scenario.

B. Optical-TTL Scheme for OLS

OLS core routers implement optical-TTL function by monitoring the OSNR of each packet. The OSNR of an optical packet will degrade as it travels through OLS router hops and fiber links in the network. The optical-TTL function detects seriously degraded packets and drops them. Particularly, when the OSNR of a packet drops below a preset threshold, the optical-TTL process will drop the packet, assuming that the packet's maximum weighted hop-count has reached. The real-time OSNR monitoring mechanism used by the optical-TTL function can also achieve optical layer performance monitoring on a packet-by-packet basis. This optical-TTL method uses label signal quality to estimate the payload signal quality.

In optical SCM labeling schemes, this will require strictly transparent wavelength converters such as four-wave-mixing and difference-frequency-generation wavelength converters which maintain both amplitude (analog and digital) and frequency domain information [24]. Since such wavelength conversion devices are not available to us at the time of experiment, we carry out a proof-of-concept optical-TTL experiment using Mach-Zehnder interferometer wavelength converters (MZI-WC) and the bit serial label.

The OLS routers use error-checking labels to achieve per-packet real time monitoring of OSNR. Because the label and the payload are transmitted in the same optical channel and experience the same impairments, payload signal quality can be estimated by the label signal quality. Each optical packet has a bit serial label that comes ahead of the payload. The label achieves real-time error checking using a bit-interleaved-parity (BIP) checking field, which is an 8-bit field at the end of the 48-bit label. Fig. 7 depicts the structure of the optical packet.

The packet source calculates the BIP value according to the first 40 bits of the label and puts the BIP value in the last 8 bits of the label. Each intermediate OLS router will read the label, recalculate a local BIP value according to the first 40 bits of the received label, and compare the local BIP value with the BIP value in the received label. If the two BIP values are not identical, it indicates that bit errors have occurred during the transmission and the packet will be dropped. This way, the BIP checking method can effectively monitor bit errors caused by the OSNR degradation.

C. OLS Edge Router Design

Edge routers implement packet aggregation and label processing capabilities to enhance the performance as an interface between the client and the OLS networks in addition to the traditional routing and policing functions. As in Fig. 8, legacy networks communicates with the OLS edge router via the legacy interfaces, for example, Fast Ethernet interfaces; while the OLS edge routers communicate with the OLS core router through OLS label and payload interfaces. Edge routers bridge the legacy protocol and the OLS protocol by inserting OLS labels to the packets at the ingress and extracting OLS labels from optical packets at the egress. Edge routers also provide different QoS/CoS/ToS policies to client applications. These policies are further mapped to the optical label fields, so that the OLS core routers can apply different policies in the OLS core networks.

Ingress Processing: As Fig. 8 illustrates, the ingress traffic is first aggregated onto one higher-speed link. Based on the headers of the packets (using Fast Ethernet as an example, the legacy protocol header includes the MAC header, the IP header, and the transmission control protocol/user datagram protocol (TCP/UDP) header), the policing/routing/buffering module then classifies the traffic to different categories and looks up for the destination ports. The categories are further mapped to different policies, which will guide the following stages to provide different QoS. The policy-based switching module delivers the packets to the OLS core network or the egress direction based on the destination ports.

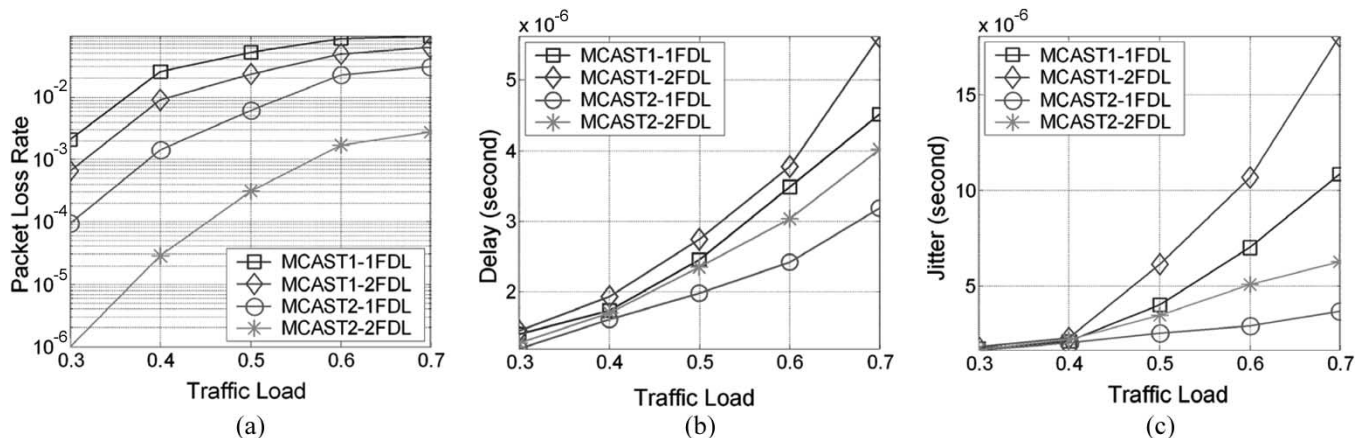


Fig. 6. Simulation results to study the performance of the multicast contention-resolution schemes; (a) packet loss rate with traffic load, (b) delay (in seconds), and (c) jitter (in seconds).

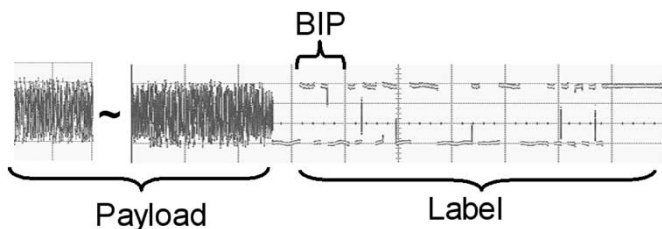


Fig. 7. Optical packet with error-checking label. Time scale: 50 ns/division. The time axis is pointing to the left, so the label is ahead of the payload. BIP: bit-interleaved parity.

Our previous work [25] indicated that, in the optical packet switching network, the packet aggregation scheme can smooth out the variations in the optical packet size distribution and achieve traffic shaping, which results in lower packet loss rate (PLR) and significantly improved TCP performance. This scheme also reduces the burstiness of Internet traffic, lowering the requirement for packet scheduling. Maximum transmission unit (MTU) adaptation occurs at the boundaries of the OLS networks to achieve high performance transport across heterogeneous underlying network technologies. In Fig. 8, the edge router implements an intelligent packet aggregation module using this algorithm. Packets belonging to different categories and destination addresses are aggregated in different queues, so that the OLS core routers can apply different policies in the OLS networks accordingly.

The aggregated packets are further delivered to the label generation module that generates the optical labels. The labels contain all the necessary information required by the OLS core routers. Using Fast Ethernet as an example of the legacy protocol, the label includes the packet length, ToS/CoS, source address, and destination address, etc. The packet length indicates the aggregated packet length; the ToS/CoS is extracted from the IP ToS/CoS field or the policing result; the addresses (both the source address and the destination address) are mapped from the original IP addresses, with fewer bits and fixed length to accelerate the table lookup performance of the OLS core routers. The edge router finally transmits the labels together with the payloads to the optical interface.

Egress Processing: For egress packets, the edge router first de-aggregates them to the original sizes. The de-aggregated

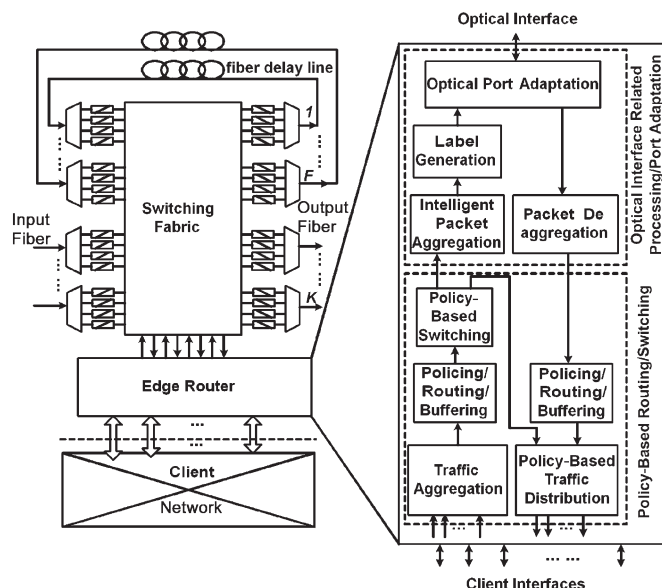


Fig. 8. Edge-router location and its internal diagram.

packets are then delivered to the policing/routing/buffering module, where they are classified to different categories and the output ports are resolved. The edge router further maps the packets to different policies to help the following stage provide different QoS, just as the ingress processing. Then the packets are delivered to the policy-based traffic distribution module. Based on the policies and destination ports of the packets, this module transmits them to the proper output ports. Finally the packets travel to the client networks through the physical interfaces.

III. OLS NETWORK AND SYSTEM DEMONSTRATION

The research on the OLS core and edge routers that combine all the features discussed in Section II is currently in progress. Here we present the experimental demonstrations of the features discussed in Section II. Section III-A discusses the experimental demonstration of an OLS core router with multicast support; Section III-B discusses the experimental

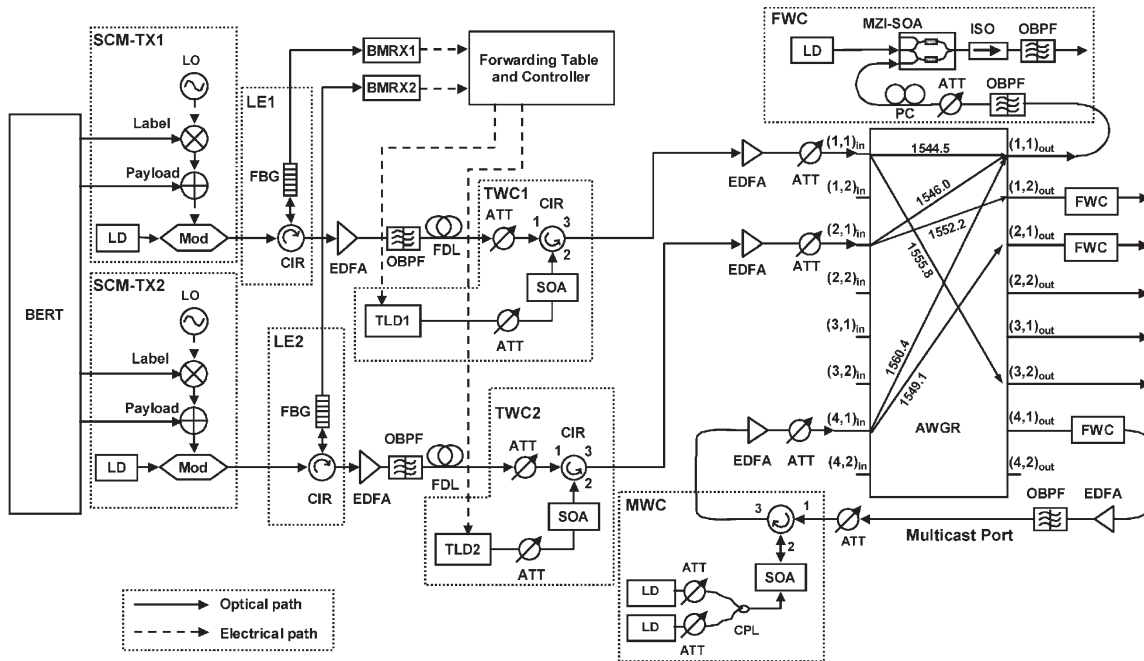


Fig. 9. Experimental setup of an OLS router with multicast function. The insets show the details of the composing modules. In the AWGR, the wavelength values for switching from a certain input to a certain output are shown. BERT: bit error rate tester; SCM TX: subcarrier-multiplexing transmitter; LD: laser diode; LO: local oscillator; MOD: modulator; LE: label extractor; FBG: fiber-Bragg grating; CIR: circulator; BMRX: burst-mode receiver; EDFA: Erbium-doped fiber amplifier; OBPF: optical bandpass filter; FDL: fiber delay line; TWC: tunable wavelength converter; ATT: variable attenuator; SOA: semiconductor optical amplifier; TLD: tunable laser diode; AWGR: arrayed waveguide grating router; FWC: fixed wavelength converter; PC: polarization controller; MZI-SOA: Mach-Zehnder interferometer wavelength converter based on SOA; ISO: isolator; MWC: multiwavelength converter; CPL: coupler.

demonstration of an optical-TTL scheme; and Section III-C discusses an end-to-end video streaming experiment with Ethernet clients, OLS edge routers and OLS core router.

A. Experimental Demonstration of an OLS Core Router With Multicast Support

Fig. 9 shows the experimental setup. It realizes two input wavelength channels in two separate fibers and one multicast port. For simplicity, this setup does not include the multiplexers, demultiplexers, fixed-length buffer and label rewriters shown in Fig. 2. Moreover, the realized MWC is a two-wavelength converter including two fixed wavelength sources instead of multiple tunable wavelength sources controlled by the switch controller.

The subcarrier-multiplexing generator (SCM TX) generates optical packets with baseband payloads at 2.5 Gb/s and double-sideband subcarrier labels at 155 Mb/s. The subcarrier frequency is 14 GHz. The label extractor (LE) utilizes a fiber-Bragg grating (FBG) as a narrow-band (0.1 nm) filter to separate the label and the payload [15]. The burst-mode receiver (BMRX) receives the label. Then the switch controller makes a switching decision according to the label content and the forwarding table. A field-programmable gate array (FPGA) realizes the switch controller with forwarding table in this experiment. During the label processing time (around 260 ns), the payload stays in the fiber delay line (FDL). According to the command from the switch control, the tunable laser (TLD) tunes and the tunable-wavelength converter (TWC) copies the payload onto the new wavelength that forwards the

payload to the desired output port of the AWGR. The fixed-wavelength converter (FWC) at the output of the AWGR converts the payload to a transmission wavelength.

If the packet is a multicast packet, the switch control will forward the payload to an available multicast port. There the MWC duplicates the payload onto multiple wavelengths that will send the packets to the multiple desired output ports of the AWGR. In this demonstration the MWC is an SOA that performs wavelength conversion by XGM.

Fig. 10(a) shows the timing diagram of the experiment. In the picture $(m, n)_{in}$ represents the n th wavelength on the m th input fiber; while $(m, n)_{out}$ represents the n th wavelength on the m th output fiber. The numbering of the label represents the destination. For example, the destination of a packet with label L1 is output fiber 1, preferably on wavelength 1, i.e., $(1, 1)_{out}$. The packet with label L3 is a multicast packet, and its destination includes output fiber 1 and 2, preferably $(1, 1)_{out}$ and $(2, 1)_{out}$. In the demonstration, packet P1 with L3 arrives at $(1, 1)_{in}$ first, occupying $(1, 1)_{out}$ and $(2, 1)_{out}$. Then packet P1' with L1 arrives at $(2, 1)_{in}$. Since P1 has passed, P1' travels to $(1, 1)_{out}$ without contention. Then P2 with L3 at $(1, 1)_{in}$ travels to $(1, 1)_{out}$ and $(2, 1)_{out}$ with no contention. But when P2' with L1 arrives, P2 is still occupying output $(1, 1)_{out}$. P2' has to go through contention resolution in the wavelength domain [4] and travels to $(1, 2)_{out}$, the second preferable wavelength on the destination fiber of P2'. Fig. 10(b) shows the packet sequences observed on a digital communication analyzer, which indicate that the router is functioning as designed. Since the TWC inverts the logic, the packets use inverted logic at the transmitter to avoid the situation that the

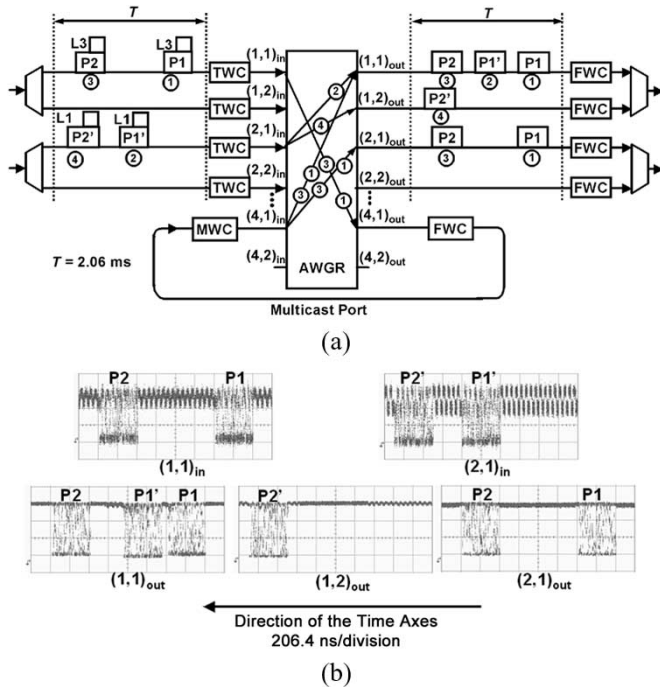


Fig. 10. (a) Timing diagram and (b) oscilloscope traces for the demonstration of an OLS router with limited multicast function. The numbers in circles show the order of packet arrival and switching. TWC: tunable wavelength converter; AWGR: arrayed waveguide grating router; FWC: fixed wavelength converter; MWC: multiwavelength converter.

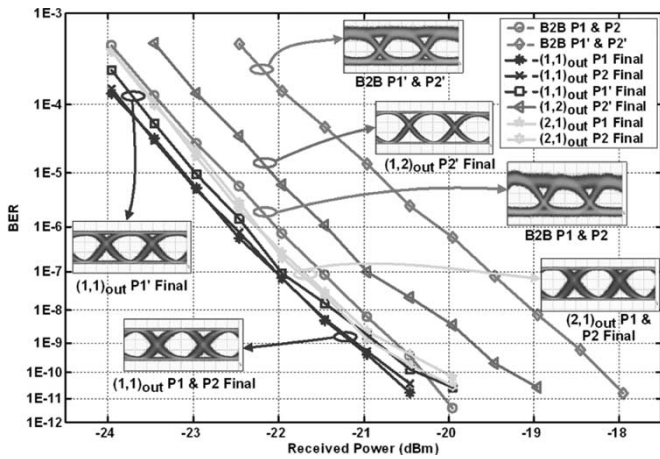


Fig. 11. Bit-error-rate measurement results and eye diagrams. B2B: back-to-back. The time scale of the eye diagrams: 100 ps/division.

switching action cuts a guard time of long “1” bits in half and delivers each section to a different output port.

Fig. 11 shows the packet-by-packet BER measurement results as well as the eye diagrams. Since P1 and P2 always travel together, their BER curves are almost overlapping. Due to crosstalk from the label, the back-to-back payload eye diagram shows thick “1” level although its BER is error free down to 1E-10. At the BER of 1E-9, most BER curves have the sensitivity between -20.7 to -20.1 dBm, except that the back-to-back P1' and P2' curves show the sensitivity of -18.6 dBm, and the P2' final output at (1,2)_{out} curve shows the sensitivity of -19.8 dBm. This power penalty is most likely due to a

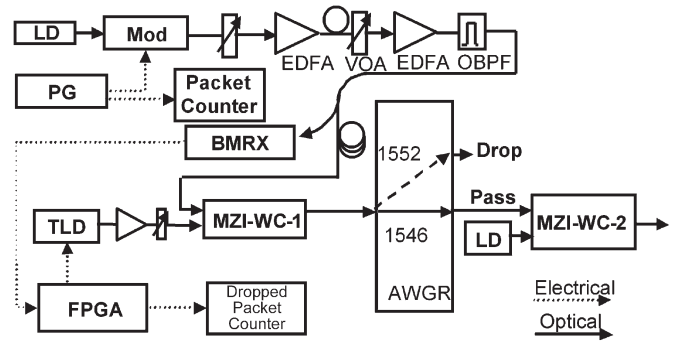


Fig. 12. Experimental setup of the demonstration of optical-TTL in an OLS router. LD: laser diode; MOD: Modulator; AWGR: arrayed-waveguide grating router; PG: pattern generator; VOA: variable optical attenuator; EDFA: erbium-doped fiber amplifier; OBPF: optical band-pass filter; BMRX: burst-mode receiver; FPGA: field programmable gate array; TLD: tunable laser diode; MZI-WC: Mach-Zehnder interferometer wavelength converter.

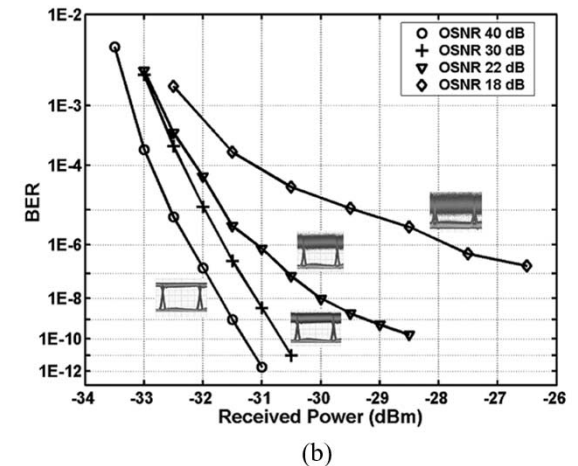
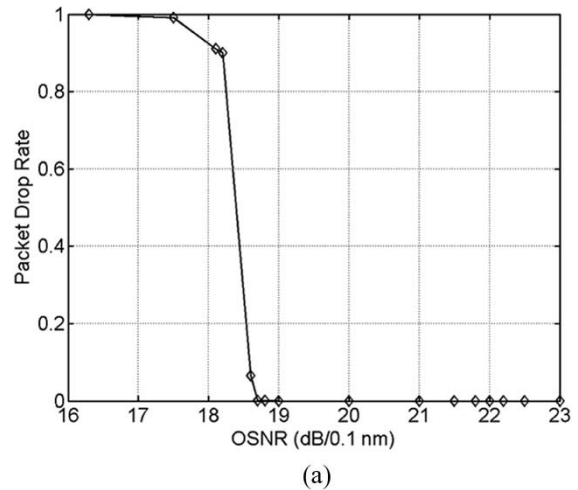


Fig. 13. Experimental results of the demonstration of the optical-TTL function in an OLS router; (a) packet drop rate, and (b) BER at different OSNR levels.

low level of crosstalk present in the switching fabric. The BER curves and the eye diagrams show that the output signals have better quality than the back-to-back signals. This is because the fixed-wavelength conversion by XPM performs reamplification and reshaping (2R) regeneration on the signal by increasing the extinction ratio and suppressing the crosstalk noise [26].

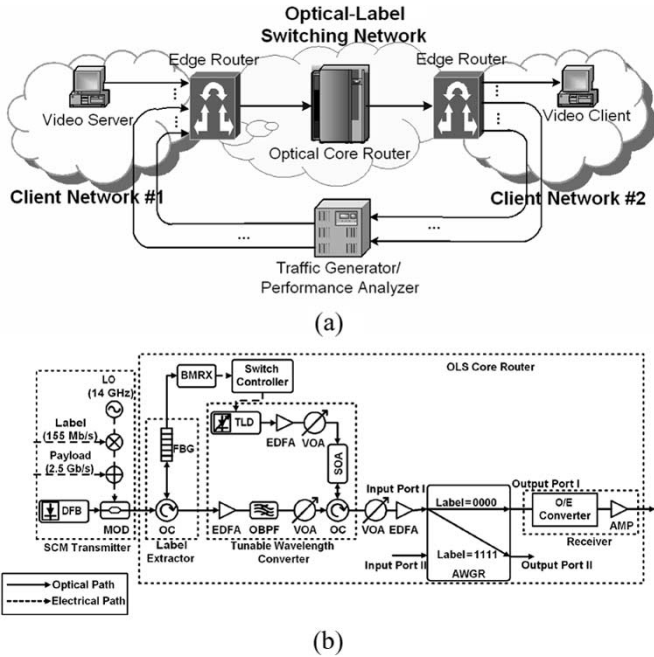


Fig. 14. Experimental setup for end-to-end video streaming with Ethernet clients, OLS edge routers, and an OLS core router; (a) network setup, and (b) setup of the OLS core router. LD: laser diode; MOD: modulator; LO: local oscillator; SCM: subcarrier multiplexing; BmRx: burst-mode receiver; FBG: fiber Bragg grating; OC: optical circulator; TLD: tunable laser diode; EDFA: erbium-doped fiber amplifier; BPF: band-pass filter; VOA: variable optical attenuator; SOA: semiconductor optical amplifier; AWGR: arrayed-waveguide grating router; AMP: amplifier.

B. Experimental Demonstration of Optical-TTL Scheme

Fig. 12 depicts the optical-TTL experiment setup. The setup includes three parts: the transmitter, the OSNR degradation emulator, and the receiver. The transmitter, which includes the parallel bit error tester, the laser diode and the modulator, generates the payload and bit serial label. The payload is at 2.5 Gb/s with Manchester line coding, while the label is 155 Mb/s non-return-to-zero (NRZ) format. The rate difference between payload and label facilitates label extraction by a low-pass filter. A packet counter will count the total number of transmitted packets. A variable optical attenuator (VOA) and an Erbium doped fiber amplifier (EDFA) emulate the OSNR degradation by adding amplified spontaneous emission (ASE) noise to the signal. Adjusting the attenuation level of the VOA will change the OSNR of the optical signal output from the EDFA. An optical band-pass filter (OBPF) with 3 dB bandwidth of 1 nm limits the total noise fed into the optical label switching system.

The OLS router constitutes the receiver part of the setup. The switching principle is the same as described in Section III-A except that this experiment uses bit serial label. At the OLS router the fiber coupler taps off 10% of the input optical power and feeds it to the BMRX, while the MZ-WC-1 receives the other 90% of the input optical power. The BMRX will convert the optical packet into electrical signal, then pass only the 155 Mb/s label signal while erasing the 2.5 Gb/s Manchester encoded payload by a low-pass filter. The electrical label signal goes to the FPGA that implements the BIP checking and

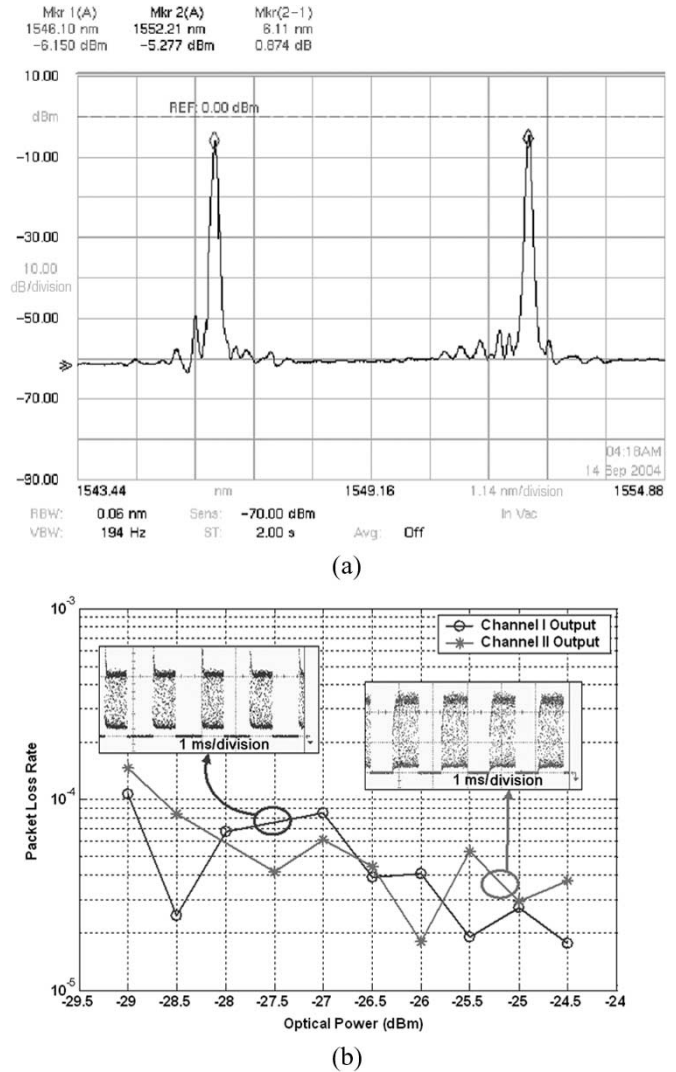


Fig. 15. Experimental results for IP-client-to-IP-client communication using edge routers and an OLS core router; (a) tunable laser-output wavelength, and (b) packet loss rate versus optical power.

optical-TTL control logic. If the BIP checking finds no errors, the FPGA will tune the wavelength of the TLD to 1546 nm. The MZI-WC-1 will convert the packet to 1546 nm and the AWGR will route the packet to the pass-through port. On the other hand, if the BIP checking finds any error, the FPGA will tune the wavelength of the TLD to 1552 nm and the AWGR will route the packet to the drop port. The FPGA will also send a pulse to dropped-packet counter when it drops a packet. The FPGA parks the TLD’s wavelength to the drop port (1552 nm) when it does not detect any input packet. At the pass-through port, MZI-WC-2 converts the wavelength to proper WDM transmission channel.

In the experiment, we adjust the two VOAs before the OBPF to vary the OSNR level of the input optical signal. The total optical power at the input of the fiber coupler is kept at a constant level regardless of the OSNR. At each OSNR level, the packet counter will record the total numbers of packets injected into the system, and the dropped-packet counter will count the dropped packets. Therefore, the packet drop rate (PDR) can be obtained at each input OSNR level.



Fig. 16. Video-streaming performance for IP-client-to-IP-client communication; (a) IP-clients back-to-back, (b) edge-routers back-to-back, and (c) using edge routers and an OLS core router.

Fig. 13(a) shows how the PDR changes with the input OSNR. When the input OSNR is 19 dB, the PDR is at 10^{-4} level. Increasing the OSNR to 21 dB or higher will lower the PDR to virtually zero—we observed no packet drop among $2^{32} - 1$ packets, which is the maximum capacity of the packet counter. On the other hand, when the OSNR is below 18 dB, the PDR is greater than 0.998, indicating that virtually all the packets are dropped. Relatively sharp transition with less than 1 dB variation in the OSNR makes this approach very attractive for optical-TTL. The above results indicate that the error-monitoring label can effectively monitor the OSNR of the incoming packets in real-time, and the OLS router drops all the packets whose OSNR is below the OSNR threshold with high-sensitivity. The experiment also investigated the BER of the system at various OSNR levels as shown in Fig. 13(b). At high OSNR levels (30 dB and 40 dB) the BER curves do not show any error floor. On the other hand, at OSNR levels around the threshold (22 dB and 18 dB), the BER curves have error floors and the eye diagrams show signal degradation, meaning that the packet has experienced significant impairment before being dropped. In this sense the BIP checking helps the cleaning up of errant packets and prevents the propagation of errant packets in the network.

C. End-to-End Video Streaming With Ethernet Clients, OLS Edge Routers and OLS Core Router

Fig. 14(a) is the experimental setup for the video-streaming demonstration. This demonstration employs an OLS router testbed with the edge routers described above. A PC-based video-streaming server (VideoLAN server [27]), together with the traffic generator, generates traffic that arrives at the ingress edge router through Ethernet ports. The ingress edge router aggregates the traffic into 2.488 Gb/s payloads and generates 155 Mb/s labels. The payload and its label are multiplexed to one optical packet using SCM and transmitted to the OLS core router. The OLS core router extracts the labels from the optical packets. Using these labels, the OLS core router applies different policies/priorities to the packets and switches the packets to the proper output port. When the packets reach the egress edge router, they will be forwarded to the PC-based video-streaming client or the performance analyzer, based on the destination addresses.

Fig. 14(b) shows the detailed OLS core router setup for the video-streaming experiment. This setup is similar to the one in the multicast demonstration except that all the traffic is unicast.

The payloads from packets that have an address “0000” in the labels are converted to 1546.0 nm and the AWGR guides them to output port I. The payloads from packets with an address “1111” are converted to 1552.2 nm and travels to output port II.

The traffic generator generates interleaved traffic destined to output port I and port II of the OLS core router. Fig. 15(a) shows the measured TLD output wavelengths, indicating the different traffic destinations and their corresponding switching channels. By adjusting the optical power, we measured the PLR for each output channel as shown in Fig. 15(b). When changing the optical power from -29 dBm to -23 dBm, there is little change in the PLR curve, indicating that the edge router–OLS core router combination can work in a relatively large power range while still providing relatively good performance. This experimental setup with IP-over-optical using OLS does not offer layer-1 testing since the edge router functions as a layer-2/layer-3 device resulting in no layer-1 testing access. Fig. 16 shows the screen captures of the video streaming demonstration at the video client by different configurations: (a) IP-clients back-to-back (i.e., the two computers are connected by an Ethernet cable directly) (b) edge-routers back-to-back (the traffic will pass through the edge router, but not the optical router), and (c) through the edge routers and an OLS core router. The video quality in Fig. 16(b) and (c) are similar, which indicates that the OLS core router did not cause noticeable degradation to the video quality of the streaming application.

IV. SUMMARY

The rapid growth of the Internet demands vast bandwidth as well as support of emerging diverse services. This paper discussed a new OLS system in support of modern features of all-optical networks. We first discussed an OLS core router architecture supporting limited multicast function. Numerical simulation studies showed that the proposed multicast contention resolution scheme 2 (*MCAST2*) with individual contention resolution had better performance over the scheme 1 (*MCAST1*). Second, we discussed the optical-TTL function to mitigate routing loop problem and to provide real-time performance monitoring. Third, we presented an OLS edge router architecture that supported end-to-end multimedia application with packet aggregation and QoS/CoS/ToS. Finally, experiments demonstrated a simple contention resolution scenario in the OLS core router with multicast capability, the optical TTL in the OLS core router that dropped deteriorated packets with a sharp threshold according to the error-checking field in the

label, and video streaming from an Ethernet-client to another Ethernet-client through two edge routers and a core router.

REFERENCES

- [1] S. Yao, B. Mukherjee, and S. Dixit, "Advances in photonic packet switching: An overview," *IEEE Commun. Mag.*, vol. 38, no. 2, pp. 84–94, Feb. 2000.
- [2] B. Meagher, G. K. Chang, G. Ellinas, Y. M. Lin, W. Xin, T. F. Chen, X. Yang, A. Chowdhury, J. Young, S. J. Yoo, C. Lee, M. Z. Iqbal, T. Robe, H. Dai, Y. J. Chen, and W. I. Way, "Design and implementation of ultra-low latency optical label switching for packet-switched WDM networks," *J. Lightw. Technol.*, vol. 18, no. 12, pp. 1978–1987, Dec. 2000.
- [3] S. J. B. Yoo, "Optical-label switching, MPLS, MPLambdaS, and GMPLS," *Opt. Netw. Mag.*, vol. 4, no. 3, pp. 17–31, May/June 2003.
- [4] Z. Pan, H. Yang, Z. Zhu, J. Cao, V. Akella, S. Butt, and S. J. B. Yoo, "Demonstration of variable-length packet contention resolution and packet forwarding in an optical-label switching router," *IEEE Photon. Technol. Lett.*, vol. 16, no. 7, pp. 1772–1774, Jul. 2004.
- [5] M. Y. Jeon, Z. Pan, J. Cao, Y. Bansal, J. Taylor, Z. Wang, V. Akella, K. Okamoto, S. Kamei, J. Pan, and S. J. B. Yoo, "Demonstration of all-optical packet switching routers with optical label swapping and 2R regeneration for scalable optical label switching network applications," *J. Lightw. Technol.*, vol. 21, no. 11, pp. 2723–2733, Nov. 2003.
- [6] J. Taylor, Y. Bansal, M. Y. Jeon, Z. Pan, J. Cao, V. J. Hernandez, Z. Zhu, Z. Wang, S. J. B. Yoo, V. Akella, T. Nady, G. Goncher, K. Ervin, K. Boyer, and B. Davies, "Demonstration of IP client-to IP client packet transport over an optical label-switching network with edge routers," presented at the 29th Eur. Conf. Optical Communication (ECOC), Rimini, Italy, 2003, paper Mo3.4.2.
- [7] V. J. Hernandez, Z. Pan, J. Cao, V. K. Tsui, Y. Bansal, S. K. H. Fong, Y. Zhang, M. Y. Jeon, S. J. B. Yoo, B. Bodtker, S. Bond, W. J. Lennon, H. Higashi, B. Lyles, and R. McDonald, "First field trial of optical label-switching and packet drop on a 477 km NTON/Sprint link," in *Postconf. Tech. Dig., Optical Fiber Communication (OFC)*, Anaheim, CA, 2002, vol. 1, pp. 168–169.
- [8] W. Hung, K. Chan, L. K. Chen, C. K. Chan, and F. Tong, "A routing loop control scheme in optical layer for optical packet networks," in *Postconf. Tech. Dig., Optical Fiber Communication (OFC)*, Anaheim, CA, 2002, vol. 1, pp. 770–771.
- [9] J. E. McGeehan, S. Kumar, D. Gurkan, S. Nezam, A. E. Willner, K. R. Parameswaran, M. M. Fejer, J. Bannister, and J. D. Touch, "All-optical decrementing of a packet's time-to-live (TTL) field and subsequent dropping of a zero-TTL packet," *J. Lightw. Technol.*, vol. 21, no. 11, pp. 2746–2752, Nov. 2003.
- [10] J. Yang, M. Y. Jeon, J. Cao, Z. Pan, and S. J. B. Yoo, "Performance monitoring by sub-carrier multiplexing in optical label switching networks," presented at the Conf. on Lasers and Electro-Optics (CLEO), Baltimore, MD, 2003, paper CThX7.
- [11] ———, "Performance monitoring in transparent optical networks using self-monitoring optical-labels," *Electron. Lett.*, vol. 40, no. 21, pp. 1370–1372, Oct. 2004.
- [12] F. Xue, Z. Pan, Y. Bansal, J. Cao, M. Y. Jeon, K. Okamoto, S. Kamei, V. Akella, and S. J. B. Yoo, "End-to-end contention resolution schemes for an optical packet switching network with enhanced edge routers," *J. Lightw. Technol.*, vol. 21, no. 11, pp. 2595–2604, Nov. 2003.
- [13] D. J. Blumenthal, B. E. Olsson, G. Rossi, T. E. Dimmick, L. Rau, M. Masanovic, O. Lavrova, R. Doshi, O. Jerphagnon, J. E. Bowers, V. Kaman, L. A. Coldren, and J. Barton, "All-optical label swapping networks and technologies," *J. Lightw. Technol.*, vol. 18, no. 12, pp. 2058–2075, Dec. 2000.
- [14] Z. Q. Zhu, V. J. Hernandez, M. Y. Jeon, J. Cao, Z. Pan, and S. J. B. Yoo, "RF photonics signal processing in subcarrier multiplexed optical-label switching communication systems," *J. Lightw. Technol.*, vol. 21, no. 12, pp. 3155–3166, Dec. 2003.
- [15] H. J. Lee, S. J. B. Yoo, V. K. Tsui, and S. K. H. Fong, "A simple all-optical label detection and swapping technique incorporating a fiber Bragg grating filter," *IEEE Photon. Technol. Lett.*, vol. 13, no. 6, pp. 635–637, Jun. 2001.
- [16] Y. Yang, J. Wang, and C. Qiao, "Nonblocking WDM multicast switching networks," *IEEE Trans. Parallel Distrib. Syst.*, vol. 11, no. 12, pp. 1274–1287, Dec. 2000.
- [17] G. N. Rouskas, "Optical layer multicast: Rationale, building blocks, and challenges," *IEEE Network*, vol. 17, no. 1, pp. 60–65, Jan./Feb. 2003.
- [18] C. W. Chow, C. S. Wong, and H. K. Tsang, "8 * 10 Gb/s multiwavelength injection locking of a FP laser diode for WDM multicast," in *Conf. Proc. IEEE Lasers and Electro-Optics Society (LEOS) Annu. Meeting*, Tucson, AZ, 2003, vol. 2, pp. 682–683.
- [19] G. Contestabile, M. Presi, and E. Ciaramella, "Multiple wavelength conversion for WDM multicasting by FWM in an SOA," *IEEE Photon. Technol. Lett.*, vol. 16, no. 7, pp. 1775–1777, Jul. 2004.
- [20] Y. Shen, J. H. Ng, C. Lu, T. H. Cheng, M. K. Rao, and D. Liu, "Single to multi wavelength conversion using amplified spontaneous emission of semiconductor optical amplifier," in *Tech. Dig. Postconf. Edition, Optical Fiber Communication (OFC)*, Anaheim, CA, 2001, vol. 1, pp. ME1-1–ME1-3.
- [21] X. Zhang, D. Huang, J. Sun, and D. Liu, "Single to 16-channel wavelength conversion at 10 Gb/s based on cross-gain modulation of ASE spectrum in SOA," *Opt. Quantum Electron.*, vol. 36, no. 7, pp. 627–634, 2004.
- [22] B. K. Ryu and S. B. Lowen, "Point process approaches to the modeling and analysis of self-similar traffic. I. Model construction," in *Proc. IEEE Information Communications (INFOCOM)*, San Francisco, CA, 1996, vol. 3, pp. 1468–1475.
- [23] Agilent Technologies. (2001, Aug.). "How can I generate traffic representative of 'Realistic' internet traffic?" *Insight* (1st ed.) [Online]. Available: http://advanced.comms.agilent.com/insight/2001-08/Questions/traffic_gen.htm
- [24] S. J. B. Yoo, "Wavelength conversion technologies for WDM network applications," *J. Lightw. Technol.*, vol. 14, no. 6, pp. 955–966, Jun. 1996.
- [25] S. Yao, F. Xue, B. Mukherjee, S. J. B. Yoo, and S. Dixit, "Electrical ingress buffering and traffic aggregation for optical packet switching and their effect on TCP-level performance in optical mesh networks," *IEEE Commun. Mag.*, vol. 40, no. 9, pp. 66–72, Sep. 2002.
- [26] T. Gyselings, G. Morthier, and R. Baets, "Strong improvement in optical signal regeneration and noise reduction through asymmetric biasing of Mach-Zehnder interferometric all optical wavelength converters," in *Proc. Integrated Optics and Optical Fiber Communication-European Conf. Optical Communication (IOOC-ECOC)*, Edinburgh, U.K., 1997, vol. 2, pp. 188–191.
- [27] VideoLAN—Free Software and Open Source Video Streaming Solution for Every OS! [Online]. Available: <http://www.videolan.org/>



Zhong Pan (S'01) received the B.S. degree in electrical engineering from Tsinghua University, Beijing, China in 2000, and the M.S. degree in electrical engineering from University of California, Davis (UC Davis) in 2002. He is currently pursuing a Ph.D. degree at UC Davis.

His research focuses on optical-label switching in optical communication networks, especially the control of the tunable laser and its application.

Mr. Pan is a Student Member of the Optical Society of America (OSA).



Haijun Yang (S'00) received the B.S. and M.S. degrees in electrical and computer engineering from the University of Science and Technology of China, Hefei, Anhui, China, in 1998 and 2001, respectively. He is currently working toward the Ph.D. degree in electrical and computer engineering at the University of California, Davis.

His current research interests include design, analysis, and implementation of switch fabric architectures, control plane electronics, and scheduling algorithms of all-optical label switching routers.



Jinqiang Yang received the B.S. and M.S. degrees in electronic engineering from Tsinghua University, Beijing, China, in 1993 and 1997, respectively, and is currently working toward the Ph.D. degree in electrical engineering at the University of California, Davis (UC Davis).

Prior to joining UC Davis, he was a Member of the Technical Staff at Bell Labs China, where he was involved in research and development work on transmission networks and multiservice edge routers. His current research interest includes next-generation optical transmission networks, network control and management systems, and performance monitoring.



Junqiang Hu received the B.S. degree in communication and electrical systems and the Ph.D. degree in communication and information systems from University of Science and Technology of China, Hefei, Anhui, China, in 1997 and 2002 respectively.

Since 2002, he has been working in a postdoctoral position in the Department of Electrical and Computer Engineering at the University of California, Davis. His research interests include router and access network architecture with an emphasis on high performance router hardware implementation.

Zuqing Zhu (S'01) received the B.S. degree from the Department of Electronic Engineering and Information Science, University of Science and Technology of China, Hefei, China, in 2001. He received the M.S. degree from the Department of Electrical and Computer Engineering, University of California, Davis, in 2003. He is working toward the Ph.D. degree at the Department of Electrical and Computer Engineering, University of California, Davis.

His research focuses on advanced switching technologies and optical communication systems for the next-generation optical networks.

Mr. Zhu is a Student Member of the Optical Society of America (OSA).

Jing Cao (S'03) received the B.S. and M.S. degrees from the Department of Electronics Engineering, Tsinghua University, Beijing, China, in 1997 and 2000, respectively, and is working toward the Ph.D. degree with the Electrical and Computer Engineering Department, University of California, Davis.

His research focuses on optical integrated devices and system integration for next-generation optical networks.

Mr. Cao is a Student Member of the Optical Society of America (OSA).

Katsunari Okamoto (M'85–SM'98–F'03), photograph and biography not available at the time of publication.

Satoru Yamano (M'03), photograph and biography not available at the time of publication.

Venkatesh Akella (S'90–M'92), photograph and biography not available at the time of publication.



S. J. Ben Yoo (S'82–M'84–SM'97) received the B.S. degree (with distinction) in electrical engineering, the M.S. degree in electrical engineering, and the Ph.D. degree in electrical engineering with minor in physics, all from Stanford University, Stanford, CA, in 1984, 1986, and 1991, respectively.

He currently serves as Professor of Electrical Engineering at the University of California at Davis (UC Davis) and Director of the UC Davis branch Center for Information Technology Research in the Interest of Society (CITRIS). His research at UC

Davis includes high-performance all-optical devices, systems, and networking technologies for the next-generation Internet. In particular, he is conducting research on architectures, systems integration, and network experiments related to all-optical label switching routers and optical code division multiple access technologies. Prior to joining UC Davis in 1999, he was a Senior Research Scientist at Bell Communications Research (Bellcore), leading technical efforts in optical networking research and systems integration. His research activities at Bellcore included optical label switching for the next-generation Internet, power transients in reconfigurable optical networks, wavelength interchanging cross connects, wavelength converters, vertical-cavity lasers, and high-speed modulators. He also participated in the advanced technology demonstration network/multiwavelength optical networking (ATD/MONET) systems integration, the OC-192 synchronous optical network (SONET) ring studies, and a number of standardization activities that led to documentations of *Generic Requirements*, GR-2918-CORE (1999), GR-2918-ILR (1999), GR-1377-CORE (1995), and GR-1377-ILR (1995) on dense wavelength division multiplexing (WDM) and OC-192 systems. Prior to joining Bellcore in 1991, he conducted research at Stanford University on nonlinear optical processes in quantum wells, a four-wave-mixing study of relaxation mechanisms in dye molecules, and ultrafast diffusion-driven photodetectors. During this period, he also conducted research on lifetime measurements of intersubband transitions and on nonlinear optical storage mechanisms at Bell Laboratories and IBM Research Laboratories, respectively.

Prof. Yoo is a Senior Member of the IEEE Lasers and Electro-Optics Society (LEOS) and a Member of the Optical Society of America (OSA) and Tau Beta Pi. He is a recipient of the DARPA Award for Sustained Excellence in 1997, the Bellcore CEO Award in 1998, and the Mid-Career Research Faculty Award (UC Davis) in 2004. He has served as Co-Chair of Technical Program Committee for APOC 2004 and APOC 2003, and Technical Program Committee Member for CLEO'2005, CLEO'2004, CLEO'2003, LEOS'2000, LEOS'1999, LEOS'1998, OECC/COIN'2004, COIN'2003, COIN'2002, NLGA'2000, and OAA'2005. He also serves as Associate Editor for IEEE PHOTONICS TECHNOLOGY LETTERS.